

Preferential Labeling of Glial and Meningeal Brain Tumors with [2-¹⁴C]Acetate

Gerald A. Dienel, David Popp, Paul D. Drew, Kelly Ball, Ali Krisht, and Nancy F. Cruz

Departments of Neurology, Anatomy, and Neurosurgery, University of Arkansas for Medical Sciences, Little Rock, Arkansas

Acetate is preferentially transported into and metabolized by astrocytes, rather than synaptosomes or neurons, and labeled acetate is used as a glial reporter molecule to assess glial metabolism and glial-neuronal interactions. Because monocarboxylic acid transporter specificity might confer a phenotype to help localize, detect, and characterize brain tumors of glial origin, use of [2-¹⁴C]acetate and [¹⁴C]deoxyglucose (a glucose analog metabolized by all brain cells) was compared in rat and human brain tumors. **Methods:** Cultured C6 glioma or U-373 glioblastoma/astrocytoma tumor cells were injected into the caudate nucleus of anesthetized CDF Fisher rats; 2–3 wk later, an intravenous pulse of [2-¹⁴C]acetate or [¹⁴C]deoxyglucose was given, and timed blood samples were drawn during the 5- or 45-min experiment, respectively. Local ¹⁴C levels in the brain were assayed by quantitative autoradiography, and acetate uptake or glucose use was calculated. Uptake and metabolism of the [¹⁴C]acetate was also assayed in C6 glioma and human surgical tumor samples in vitro. **Results:** [¹⁴C]Acetate uptake into rat brain C6 tumors was 9.9 ± 2.1 mL/100 g/min, compared with 3.9 ± 1.0 mL/100 g/min in contralateral tissue ($n = 6$; $P < 0.001$), and was much higher than that into other brain structures (e.g., 5:1 for white matter and 2:1 for cortical gray matter). Glucose use in C6 tumors was 111 ± 34 μ mol/100 g/min, versus 81 ± 5 μ mol/100 g/min in contralateral tissue ($n = 6$; $P = 0.08$); no left-right differences in glucose use or acetate uptake were seen in other brain structures. The tumor-to-contralateral-tissue ratio for acetate (2.3 ± 0.3) exceeded that for deoxyglucose (1.4 ± 0.5) ($P < 0.05$), indicating that acetate is a sensitive C6 glioma marker. [¹⁴C]Acetate uptake also demarcated a few 3-wk-old C6 tumors that had unlabeled necrotic cores. U-373 tumors were smaller than C6 tumors in rat brain and were detected equally well with [¹⁴C]acetate and [¹⁴C]deoxyglucose. In vitro uptake of [¹⁴C]acetate into human glioblastoma or meningioma tumors was higher than uptake into pituitary adenoma. Rat C6 and human tumors with high uptake metabolized acetate to acidic compounds and amino acids. **Conclusion:** Tumor imaging with radiolabeled acetate can help to localize and classify brain tumors. Transporter and metabolic substrate specificity are traits that can be exploited further for in vivo imaging of brain glial tumors.

Key Words: acetate; brain; tumor; imaging

J Nucl Med 2001; 42:1243–1250

Critical issues in treatment of human brain tumors include localization of the tumor and any metastases, identification of tumor type, estimation of tumor growth rate, determination of tumor-tissue boundaries (e.g., for planning surgical removal), and monitoring therapeutic intervention (1,2). Metabolic brain imaging uses radiolabeled tracers, including deoxyglucose, methionine, nonmetabolizable amino acids, and ions, to evaluate dynamic (as opposed to structural) properties of tumors (1,2). Unfortunately, none of these tracers can distinguish cell type, although such a capability could aid in the noninvasive diagnosis and treatment of tumors.

Early studies of brain metabolism using various substrates established compartmentation of metabolism and metabolic specialization of the 2 major cell types in brain: neurons and astrocytes (3). Acetate is widely used as a tool for in vivo study of glial-neuronal interactions and trafficking of metabolites from glia to neurons in the brain (4,5). Rapid uptake and preferential metabolism of labeled acetate by astrocytes, rather than by neurons, is attributed to transport (6) and has been confirmed by in vitro and in vivo studies (5,7–9). If glia-derived brain tumors possess a monocarboxylic acid transporter with a substrate specificity similar to that of astrocytes, radiolabeled acetate might be a useful imaging tracer to help detect and localize glial tumors (Fig. 1).

Current studies in our laboratory to assess the autoradiographic use of [¹⁴C]acetate as a glial reporter molecule and to evaluate astrocytic responses to normal sensory stimulation and pathophysiologic conditions in brain in vivo found a relatively low rate of acetate uptake and small increase during physiologic stimulation (10). A low background activity and insensitivity to brain activation would be an advantage for tracer accumulation-based detection of brain tumors because a high tumor-to-tissue uptake ratio, compared with the ratio for glucose metabolism tracers, would provide greater sensitivity in detecting small tumors. The purpose of this study was, therefore, to determine if [¹⁴C]acetate preferentially labels glial tumors grown in rat brain in vivo and in human tumor explants; preliminary results have been reported (11).

MATERIALS AND METHODS

Materials

[2-¹⁴C]Acetate and 2-[1-¹⁴C]deoxy-D-glucose ([¹⁴C]DG) (specific activities, 2,035 MBq/mmol) were purchased from NEN Life

Received Jan. 16, 2001; revision accepted Apr. 9, 2001.

For correspondence or reprints contact: Gerald A. Dienel, PhD, Department of Neurology, Slot 500, University of Arkansas for Medical Sciences, 4301 W. Markham St., Little Rock, AR 72205.

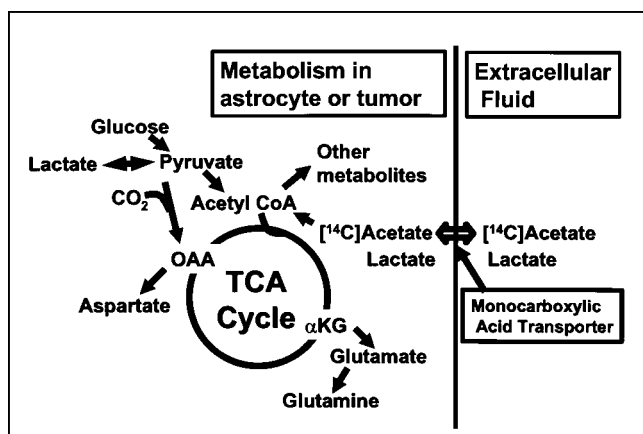


FIGURE 1. Model for metabolic trapping of $[^{14}\text{C}]$ acetate involves preferential uptake into astrocyte or tumor from extracellular fluid through unidentified isoform of monocarboxylic acid transporter. Stimulation of acetate uptake into cell might be enhanced by high rate of glycolysis and lactate efflux, that is, transacceleration of acetate uptake by lactate export (6). Once in cell, acetate can be converted to acetyl coenzyme A (CoA) and metabolized further by various pathways, including entry into tricarboxylic acid (TCA) cycle, leading to incorporation of ^{14}C into various acidic compounds, including α -ketoglutarate (α KG) and oxaloacetate (OAA). Rapid transamination reactions would cause labeling of TCA cycle–derived amino acids, glutamate, glutamine, and aspartate. With longer experimental times, label derived from acetate would also be incorporated into lipid and protein.

Science Products (Boston, MA). Male CDF Fisher rats weighing 250–275 g were obtained from Charles River (Wilmington, MA). Tumor cell lines were obtained from American Type Culture Collection (ATCC, Rockville, MD) and included C6 rat glioma (ATCC CCL-107) and U-373 human glioblastoma/astrocytoma (ATCC HTB-17).

Experimental Procedures

C6 and U-373 tumor cells were grown under standard culture conditions using media specified by ATCC. Implantation of tumor cells or agar vehicle into the brain of anesthetized rats was performed as described (12), and tumors were grown in vivo for 2–3 wk. On the experimental day, the rats were anesthetized, cannulae were inserted into an artery and vein, and 3 h were allowed for recovery. Arterial blood gases and pH, blood pressure, hematocrit, body temperature, and arterial blood glucose and lactate levels were determined before the experiment.

Metabolic labeling was initiated by intravenous injection of a pulse (3,700 kBq/kg) of $[^{14}\text{C}]\text{DG}$ or $[^{14}\text{C}]\text{acetate}$, and timed arterial blood samples were drawn to determine the integrated specific activity in plasma for $[^{14}\text{C}]\text{DG}$ or the time–activity integral for $[^{14}\text{C}]\text{acetate}$. At the end of the experimental interval (45 min for $[^{14}\text{C}]\text{DG}$ or 5 min for $[^{14}\text{C}]\text{acetate}$), the rats were killed (pentobarbital, 100 mg/kg), and the brains were processed for quantitative autoradiography (13). Local ^{14}C levels (Bq/g tissue) were determined by computer-assisted densitometry, and rates of glucose use ($\mu\text{mol/g/min}$) were calculated (13). Net acetate uptake (mL/g/min) was calculated by dividing the tissue ^{14}C content by the plasma time–activity integral; this is a minimal value because the plasma integral exceeds that of the true brain acetate precursor pool. In some experiments, tissue sections near those used for autoradiog-

raphy were stained with thionin or antibodies for glial fibrillary acidic protein (GFAP, an astrocyte marker) for histologic analysis. Animal procedures were reviewed and approved by the institutional animal care and use committee.

In Vitro Acetate Uptake Assays

To establish the experimental conditions to assay $[^{14}\text{C}]\text{acetate}$ uptake into human tumor samples, preliminary experiments were first performed on rat brain containing 2-wk-old C6 glioma tumors. The rats were decapitated, and the brain was removed, placed into ice-cold artificial cerebrospinal fluid (aCSF) (123 mmol/L NaCl, 5 mmol/L KCl, 2.5 mmol/L CaCl_2 , 1.2 mmol/L MgCl_2 , 1.2 mmol/L NaH_2PO_4 , and 26 mmol/L NaHCO_3), cut into 550- μm -thick slices (14) with a Vibroslice (World Precision Instruments, Sarasota, FL), and preincubated for 60 min at 37°C in aCSF containing 10 mmol/L glucose and 3.1% dextran to minimize slice swelling (14), with continuous bubbling with a humidified mixture of 95% oxygen and 5% CO_2 . Then, the samples were transferred to an incubation medium consisting of aCSF containing 3.1% dextran, $[^{14}\text{C}]\text{acetate}$ (7.4 kBq/mL), and 0.2 mmol/L unlabeled acetate for 10–40 min at 37°C . After labeling, the slices were quickly rinsed 3–4 times in aCSF containing 0.2 mmol/L unlabeled acetate to displace $[^{14}\text{C}]\text{acetate}$ from the surface of the slice. The slices were then frozen and cut into 20- μm -thick sections, and ^{14}C levels in each serial section were determined by quantitative autoradiography and averaged to obtain the value for each slice. Net acetate uptake ($\mu\text{mol/g/min}$) was calculated by dividing the tissue ^{14}C content by acetate specific activity and labeling time.

Fourteen surgically removed samples of human brain tumors and 1 “gliotic tissue” removed after a gunshot wound were immediately placed into ice-cold sterile saline and transferred to the laboratory within 15 min. Most human tumors were too fragile to be cut with a Vibroslice and so were cut manually into 0.5- to 1.0-mm-thick slices. Within 30 min, the tumor slices were preincubated and 1 or more slices of each tumor were assayed for net $[^{14}\text{C}]\text{acetate}$ uptake. The slices were then washed, frozen, and cut into 20- μm -thick serial sections or extracted to assess the metabolism of acetate. Global ^{14}C levels were determined by quantitative autoradiography for each serial section of each slice and averaged to obtain a value for that slice; ^{14}C levels in the obvious focal areas of intense labeling (i.e., hot spots) were similarly determined. Mean net uptake rates were calculated for each slice as a whole and for the hot spots in the slice; uptake was approximately linear with time, and values for each tumor are reported as the mean rate for all slices. The use of human tumor samples was reviewed and approved as an exempt protocol by the local human research advisory committee.

Fractionation of $[^{14}\text{C}]\text{Metabolites}$ of $[2\text{-}^{14}\text{C}]\text{Acetate}$

Metabolism of $[^{14}\text{C}]\text{acetate}$ was assessed in three 2-wk-old C6 glioma tumors and 6 in vitro human tumors that were large enough for further analysis. In brief, rats were pulse labeled in vivo, anesthetized, and decapitated; the brain was rapidly removed and placed in ice-cold aCSF; and the tumor and contralateral cerebral cortical tissue were dissected out and frozen in isopentane within 1.5 min after decapitation. Frozen samples of rat tumor and contralateral brain tissue or in vitro–labeled human tumors were extracted with perchloric acid (15) and then fractionated on DOWEX 50 H^+ columns (Bio-Rad Laboratories, Hercules, CA) to separate amino acids plus basic compounds (eluent fraction) from acidic plus neutral compounds (effluent fraction). Acetate was removed from nonvolatile acidic metabolites by acidifying ali-

quots ($\text{pH} < 1$) to convert acetate to the free acid, which was then removed by freeze drying. Portions of each fraction were assayed for their ^{14}C content. Transient postmortem metabolism would be expected, but energy failure would quickly block incorporation of ^{14}C acetate into acetyl coenzyme A and interconversion of tricarboxylic acid cycle intermediates that require oxidation of reduced nicotinamide adenine dinucleotide.

RESULTS

Imaging Glioma Tumors Grown in Rat Brain In Vivo

Physiologic variables in all rats were similar and within the reference range. C6 glioma tumors grown for 2 or 3 wk in rat brain were readily detected with ^{14}C -labeled deoxyglucose and acetate as metabolic tracers (Fig. 2). Labeling of the C6 tumors assayed with either tracer was heterogeneous, with zones of high and low uptake (Figs. 2A–2C); the thionin-stained sections in Figures 2A and 2D show darkly stained regions corresponding to the high density of

the tumor cells, in comparison with normal brain tissue; these thionin-stained regions approximate the zones of high tracer uptake but are not exactly coincident because of the irregular tumor shapes and staining of sections that are nearby but different from those used for autoradiography. Most tumors were localized in the caudate nucleus and cortex (Fig. 2A), but some showed extracerebral growth (Fig. 2B). Both intracerebral and extracerebral portions of the tumors were readily visualized by the metabolic tracers, indicating adequate delivery of the tracer through blood to the tumors. Labeling by acetate was, in general, more uniform throughout the normal brain than was labeling by deoxyglucose. In some brains, prominent labeling of the lateral ventricle by ^{14}C acetate was evident (Figs. 2B2 and 2B3), presumably because of very high uptake and trapping in the choroid plexus. A few 3-wk-old tumors were examined, and these had necrotic zones that were not labeled by

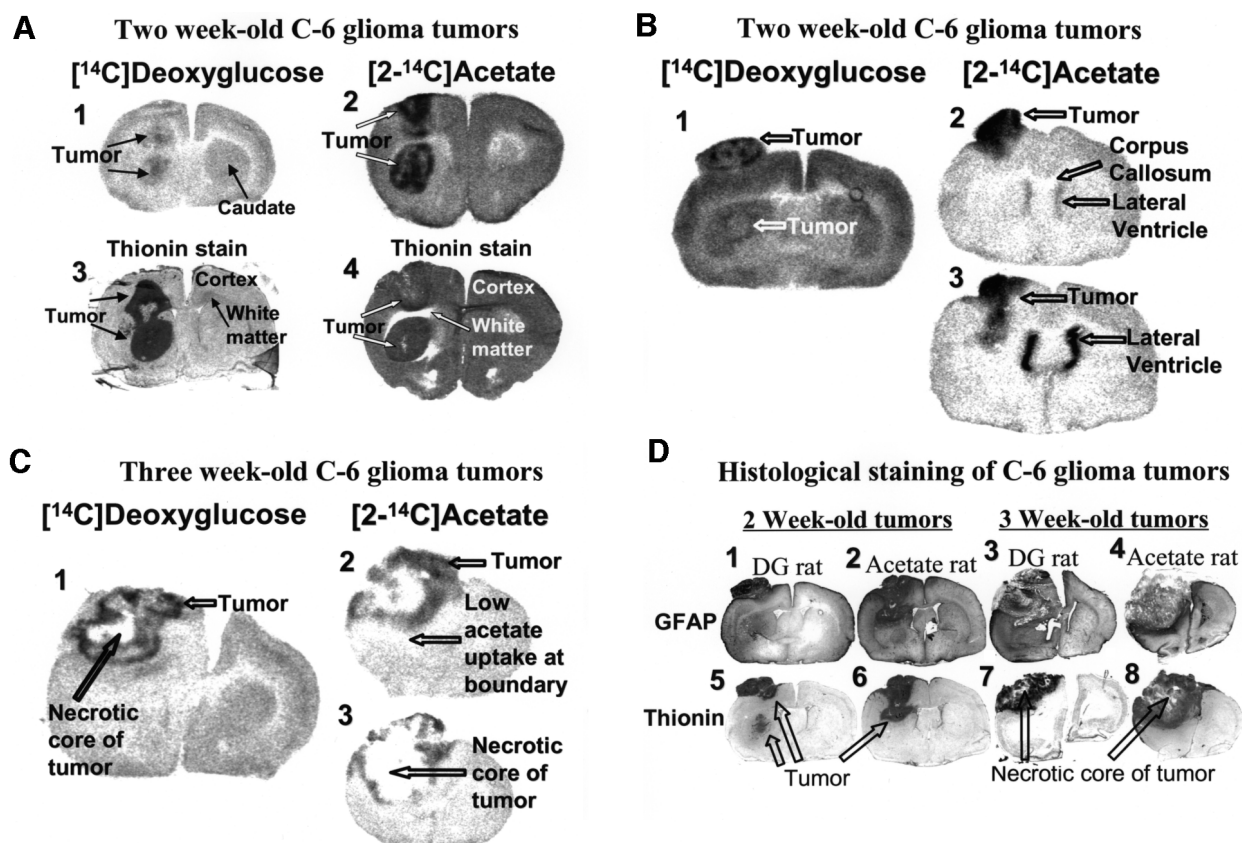


FIGURE 2. Metabolic labeling of C6 glioma tumors with ^{14}C acetate is illustrated in tumors grown in rat brain in vivo for 2 (A and B) or 3 (C) wk and assessed by autoradiography (A–C) and histologic staining (A and D). Autoradiographs show heterogeneous metabolic labeling by ^{14}C deoxyglucose (DG) and ^{14}C acetate in 2-wk-old intracerebral (A1 and A2) and extracerebral (B1–B3) tumors and in 3-wk-old necrotic tumors (C1–C3); different serial sections of same tumor (B2 and B3; C2 and C3) illustrate varied labeling of larger tumors, particularly in necrotic tumor. Thionin staining of sections near those used for autoradiography detects regions of densely packed cells in tumor (A3 and A4; D5–D8) compared with normal tissue. GFAP is marker for reactive astrocytes and also stains portions of C6 glioma tumors and zones surrounding tumors (D1–D4). Stained sections in D correspond to autoradiograph sections taken from same animals (B and C). Note low labeling of white matter (i.e., corpus callosum and subcortical white matter) by deoxyglucose and acetate (A–C), high labeling of lateral ventricle by acetate (B2 and B3), and relatively low labeling by acetate in boundary zone ventral to necrotic tumor (C2), which appears to coincide with GFAP-rich zone in 3-wk-old tumor (D4). Values for glucose use and net acetate uptake are presented in Table 1.

TABLE 1
Glucose Use and Acetate Uptake in Tumors
and Rat Brain Tissue In Vivo

Brain region	Glucose use ($\mu\text{mol}/100 \text{ g}/\text{min}$)	Net acetate uptake ($\text{mL}/100 \text{ g}/\text{min}$)
Rat C6 glioma	$111.0 \pm 34.0^*$	$9.9 \pm 2.1^\dagger$
Contralateral brain tissue	81.0 ± 5.0	3.9 ± 1.0
Tumor/contralateral tissue	1.4 ± 0.5	$2.3 \pm 0.3^\ddagger$
Human U-373		
glioblastoma/astrocytoma	$112.0 \pm 27.0^*$	$4.2 \pm 0.1^\dagger$
Contralateral brain tissue	86.0 ± 11.0	2.8 ± 0.5
Tumor/contralateral tissue	1.3 ± 0.2	1.5 ± 0.2
Rat gray matter [§]		
Frontal cortex		
Right	82.4 ± 7.4	4.8 ± 0.7
Left	77.3 ± 6.5	6.9 ± 2.0
Sensorimotor cortex		
Right	84.4 ± 7.8	4.6 ± 1.2
Left	75.4 ± 3.7	4.3 ± 1.4
Caudate nucleus		
Right	83.6 ± 8.5	3.3 ± 0.4
Left	76.6 ± 9.6	3.7 ± 0.8
Sensory cortex		
Right	87.6 ± 7.5	4.2 ± 0.8
Left	87.5 ± 7.9	4.1 ± 0.9
Rat white matter [§]		
Forceps minor corpus callosum		
Right	35.6 ± 2.8	2.2 ± 0.6
Left	35.5 ± 2.3	2.3 ± 0.2
Genu of corpus callosum		
Right	35.2 ± 2.4	2.5 ± 0.5
Left	32.0 ± 1.2	2.3 ± 0.4

* $P < 0.09$ vs. contralateral tissue.

$^\dagger P < 0.005$ vs. contralateral tissue.

$^\ddagger P < 0.05$ vs. deoxyglucose tumor-to-tissue ratio.

§ Data are from rats implanted with C6 tumors.

Data are mean \pm SD (C6 tumors: $n = 6$ for glucose use, $n = 7$ for acetate uptake; U-373 tumors: $n = 4$ per group for glucose use and acetate uptake).

either tracer (Fig. 2C). Comparison of the autoradiographic labeling patterns obtained in 2- to 3-wk-old tumors (Figs. 2A–2C) with nearby GFAP- or thionin-stained sections (Figs. 2A and 2D) indicated that high metabolic activity was mainly in tumor tissue, not in the necrotic zone of the tumor or in the boundary zone of tissue surrounding the tumor. In a few sections, cells that were highly stained with GFAP (presumably reactive astrocytes) and located at the tumor boundary (Figs. 2D4 and 2D8) appeared to have a lower uptake of [^{14}C]acetate than did the tumor (Fig. 2C2).

Net uptake of [2- ^{14}C]acetate into 2-wk-old C6 glioma tumors exceeded values obtained in contralateral normal cortical or striatal brain tissue by 2.3-fold (Table 1). Tissue contralateral to the tumor could include caudate nucleus, corpus callosum, or cerebral cortex, depending on the size and location of the tumor. The C6 glioma tumors also had higher rates of

glucose use than did other brain structures, but [^{14}C]acetate labeling yielded a higher tumor-to-tissue uptake ratio (Table 1), indicating that acetate is a more sensitive labeling reagent for C6 glioma tumors. Normal brain regions did not exhibit left–right differences in metabolic labeling with either tracer unless portions of the tumor were present in the tissue (Fig. 2; Table 1). Left–right differences for the agar vehicle were $<10\%$ at the injection site ($n = 2$ for acetate and deoxyglucose).

In separate groups of rats ($n = 5$ per group) in which C6 tumors were implanted, oral dosing with 2-methoxyestradiol (80 mg/kg in olive oil), an antiangiogenesis compound, or vehicle for 9 d beginning on the fifth day after implantation did not significantly alter the tumor volume or [^{14}C]acetate uptake in C6 tumor or brain tissue (data not shown). In vehicle-treated rats, the C6 tumor-to-tissue ratio for acetate was 2.0 ± 0.7 and tumor volume, estimated by summing the area of [^{14}C]labeled tumor in serial autoradiographic sections, was $33.6 \pm 19.3 \text{ mm}^3$.

U-373 human-derived glioblastoma/astrocytoma tumors were also grown in CD Fisher rats to assess detection of a different tumor cell line by [^{14}C]acetate. The U-373 tumors were much smaller than the C6 glioma tumors but were readily detected by autoradiography with both [^{14}C]acetate and [^{14}C]DG (Table 1). Glucose use rates were similar in the C6 and U-373 tumors, whereas acetate uptake into the U-373 tumors was, for unknown reasons, about half that into the C6 gliomas (Table 1); the tumor-to-tissue uptake ratios obtained with the 2 metabolic tracers were similar in U-373 tumors (Table 1). The mean acetate uptake values for contralateral tissue in the brains with U-373 tumors were somewhat lower than in the brains with C6 tumors, perhaps because of differences in tumor location and blood acetate levels; blood lactate levels in the 2 groups were similar.

In vivo metabolism of [^{14}C]acetate and its incorporation into amino acid pools was rapid and similar in normal rat cerebral cortex and 2-wk-old C6 glioma tumors (Table 2).

TABLE 2
Metabolism of [^{14}C]Acetate in C6 Glioma Tumors
and Rat Brain

Fraction	Percentage of total ^{14}C in acid extract (mean \pm SD, $n = 3$)	
	C6 tumor	Contralateral cerebral cortex
Unmetabolized [^{14}C]acetate	5.0 ± 2.9	5.5 ± 1.9
Acidic + any neutral metabolites	37.0 ± 2.2	29.1 ± 0.8
Amino acids + any basic metabolites	59.6 ± 3.1	68.7 ± 2.9
Total metabolized	96.6 ± 2.6	97.7 ± 2.7

Proportions of labeled compounds recovered in acidic and amino acid fractions were not significantly different in tumor and contralateral tissue ($P > 0.08$, t test).

Approximately 95% of the total ^{14}C was recovered as metabolites at the end of the 5-min experimental period. Non-volatile acidic (plus any neutral) metabolites, presumably mainly tricarboxylic acid cycle intermediates, accounted for 30%–40% of the ^{14}C in the acid extract, whereas the amino acid fraction (plus any basic compounds) contained 60%–70%. Comparable results were obtained in funnel-frozen brain of non-tumor-bearing rats (G.A. Dienel et al., unpublished data, 2000).

The contribution of ^{14}C in residual blood in brain to the autoradiographic assay is negligible. Calculations similar to those we used to assess the contribution of ^{14}C hexose levels in residual blood in freeze-blown brain (16) indicate that blood-borne ^{14}C acetate would contribute <3% of the label in normal brain tissue (Fig. 2; Tables 1 and 2), assuming 2.6% blood in brain (17).

^{14}C Acetate Uptake into Human Brain Tumors In Vitro

Net uptake of ^{14}C acetate into human tumor slices was first assayed as a function of time by autoradiography to simulate an imaging procedure and to compare total and local uptake of ^{14}C acetate in slices of 14 tumors and 1 gliotic tissue sample shortly after surgical removal from patients. ^{14}C uptake into most of the human tumor samples was approximately linear with time for 10–40 min of incubation at 37°C but was not homogeneous, that is, all tumors had focal hot spots (Fig. 3) that had, on average, 40%–50% greater ^{14}C uptake than the mean value for that tumor (Table 3). Mean net uptake values for glioblastoma and meningioma tumors were 3- to 6-fold higher than those for pituitary adenoma, 1 of the 2 oligodendroglioma samples, and 1 sample of gliotic tissue (Table 3).

Metabolism of ^{14}C acetate could be assessed in only 6 of the 14 human tumors because of the small sizes of most samples. Mean (\pm SD) acetate uptake into glioblastoma and meningioma slices was 0.22 ± 0.11 and 0.26 ± 0.21 nmol/min/mg protein, respectively, and incorporation into metabolites was 0.16 ± 0.12 and 0.20 ± 0.20 nmol/min/mg

TABLE 3

Net Uptake of ^{14}C Acetate into Human Tumor Samples Assayed In Vitro

Tumor type/sample	Acetate uptake ($\mu\text{mol}/100 \text{ g}/\text{min}$)	
	Whole tumor	Hot spots
Glioblastoma		
1 high grade	1.90	2.60
2 recurrent	0.56	0.93
3 low grade	0.38	0.56
4 recurrent	1.20	1.60
5 recurrent	0.55	0.89
6 unknown grade	0.42	0.80
Mean \pm SD ($n = 6$)	0.84 ± 0.60	1.20 ± 0.76
Meningioma		
1	0.77	1.30
2	0.52	0.83
3	0.24	0.42
4	1.60	2.40
Mean \pm SD ($n = 4$)	0.78 ± 0.58	1.20 ± 0.80
Pituitary adenoma		
1	0.22	0.36
2	0.27	0.41
Oligodendroglioma		
1	0.67	1.00
2	0.27	0.39
Gliotic tissue		
	0.13	0.23

Data are average uptake into entire slice for all slices at all incubation times for each tumor and average for hot spots in same tumors.

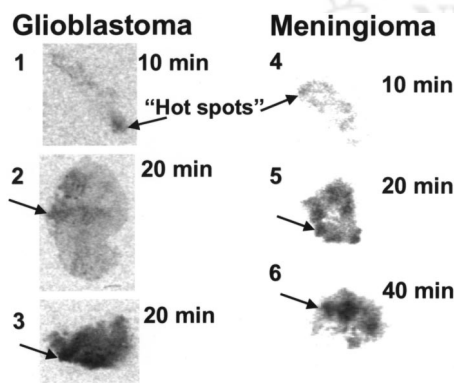


FIGURE 3. Representative 20- μm -thick sections of slices of human glioblastoma (1–3) or meningioma (4–6) tumors that were incubated in vitro with ^{14}C acetate for 10–40 min show heterogeneous labeling. Arrows indicate local areas of more intense uptake of tracer.

protein, respectively. Because the net uptake rates for the individual tumors were quite variable, the percentage conversion of acetate to products is presented for each tumor in Table 4. Significant levels of labeled metabolites were detectable within 10 min in all but 1 sample (i.e., glioblastoma 1), which had a longer lag than all the others. More than 50% of the ^{14}C was recovered in metabolites at either 10 or 20 min in 8 of 11 tumor slices, and both glioblastoma and meningioma tumors rapidly incorporated ^{14}C into amino acids. The proportions of ^{14}C recovered in the amino acid fractions ranged from values equal to or up to twice those in the acidic metabolite fractions (Table 4). In nearly all samples, the unmetabolized ^{14}C acetate fell with increasing incubation time, so the precursor contributed a progressively lower fraction to the total ^{14}C in the autoradiographs of the slices (Fig. 3).

DISCUSSION

The results of this study reveal 2 major points. First, ^{14}C acetate imaging can be used to detect, localize, and measure the volume of experimental glioma tumors in rat brain in vivo. Second, ^{14}C acetate uptake and metabolism in rat and human brain tumors in vitro is selective, and tumor metabolism of acetate includes incorporation of label into acidic compounds and amino acids, which should en-

TABLE 4
In Vitro Metabolism of [^{14}C]Acetate by Human Tumors

Tumor type	Tumor sample	Incubation time (min)	Percentage of total ^{14}C in acid extract		
			Unmetabolized [^{14}C]acetate	Acidic + any neutral metabolites	Amino acids + any basic metabolites
Glioblastoma	1	10	101	2	3
		20	63	12	29
	2	10	76	10	16
		20	20	25	52
	3	10	37	17	51
		20	20	17	59
Meningioma	1	10	58	22	24
		40	41	26	27
	2	10	42	30	29
		20	22	35	47
	3	10	11	29	60
		20	12	30	58

Protein content of acid-extracted slices was 0.06–1.2 mg per sample. Recovery of ^{14}C in fractions of acid extract was 101% \pm 4%.

hance label trapping within a tumor. [^{14}C]Acetate uptake and trapping in various glial tumors differ considerably; labeling of C6 glioma tumors was twice that of U-373 human glial tumors, and net uptake into human glioblastoma and meningioma tumors varied over a 5- to 8-fold range. The sensitivity of [^{14}C]acetate in detecting tumors, based on the tumor-to-contralateral-tissue ratio, was as good as or better than that of [^{14}C]deoxyglucose. [^{14}C]acetate labeled the C6 tumor but not the necrotic zones in the few older (i.e., 3-wk) tumors, and tumor labeling appeared to exceed that of the dense zone of reactive astrocytes near the tumor-tissue interface (Figs. 2C and 2D), raising the possibility that reactive astrocytes near tumors might not be as prominently labeled by acetate as is the tumor.

The rate of metabolism of acetate in normal rat brain is lower and more homogeneous than the local rates of glucose use, thereby providing a lower, more stable background for tumor detection. Rat plasma acetate levels are approximately 0.3 mmol/L (18), and minimal rates of net acetate uptake in rat brain, estimated by dividing net uptake values in Table 1 by 0.3 $\mu\text{mol/mL}$, are at least 5%–10% of the rate of glucose use. The presence of any labeled metabolites of [$2\text{-}^{14}\text{C}$]acetate in blood was not assessed in this study ($^{11}\text{CO}_2$ is rapidly produced from [$1\text{-}^{11}\text{C}$]acetate (19)); these would inflate the plasma time-activity integral and contribute to underestimation of acetate use.

Delivery, uptake, and trapping of labeled acetate in a brain tumor can be influenced by the extent of angiogenesis, blood-brain barrier integrity, isoforms of the monocarboxylic acid transporter at the cell surface, tumor oxygenation, and metabolism of labeled products. Extensive labeling of the tumors in rat brain in vivo indicates adequate delivery of the tracer through blood, but local factors cause heterogeneity of labeling within the tumors. Rapid incorporation of

[^{14}C]acetate into amino acids in rat brain and C6 glioma tumors is consistent with early studies of metabolic compartmentation in normal brain. [$1\text{-}^{14}\text{C}$]Acetate is quickly incorporated into glutamate and glutamine (3,20,21), and the ^{14}C incorporated into these amino acids, as well as total radioactivity in brain, rises for at least 15 min (20) and then falls by 30 min (21). With increasing time, progressively higher amounts of [^{14}C]acetate would be incorporated into protein and lipid (20).

Acetate uptake into tumor cells might be influenced by glycolytic metabolism of glucose and export of lactate from the cell, a trait that contributes to high tumor labeling by deoxyglucose (1,2). C6 glioma cells are glycolytic but also perform oxidative metabolism (22,23), and the current study clearly shows that C6 glioma cells growing in brain in vivo do metabolize acetate to nonvolatile acidic compounds (e.g., tricarboxylic acid cycle intermediates) and amino acids (Fig. 1), indicating an active tumor oxidative pathway. Tumors have variably perfused microvasculature (24) and heterogeneous O_2 levels (25,26), but the degree of hypoxia necessary to impair acetate metabolism is not known. Conceivably, use of oxygen or carbogen (95% O_2 /5% CO_2) during acetate labeling might increase oxidative metabolism and enhance imaging of tumors. On the other hand, tumor glycolysis and lactate export might be critical factors in acetate accumulation because acetate uptake into astrocytes is stimulated by lactate efflux, that is, transacceleration (6). Thus, high lactate output from a glycolytic tumor might, in fact, markedly enhance acetate influx.

An important issue for brain imaging is loss of contrast between normal and abnormal tissue because of efflux or spreading of labeled metabolites. For example, spreading of $^{14}\text{CO}_2$ and its trapping by unlabeled tissue bicarbonate could diminish the contrast at the tumor-tissue boundary. The

experimental period in this study was only 5 min to minimize product loss and spreading; [2-¹⁴C]acetate was used instead of [1-¹⁴C]acetate so that less ¹⁴C would be lost through decarboxylation reactions. Incorporation of ¹⁴C into the large amino acid pools in brain should retard this process because dilution in the larger unlabeled amino acid pools will reduce the specific activity of labeled products. To summarize, selective uptake, incorporation into amino acids, and relatively low labeling of normal brain are attributes supporting the usefulness of acetate as a tumor marker.

This initial study of in vitro [¹⁴C]acetate uptake into 14 human brain tumors and 1 sample of gliotic tissue shows, first, that labeling of glioblastoma and meningioma tumors by acetate is, on average, 3- to 6-fold higher than that of pituitary adenoma and gliotic tissue, with larger differences in the focal hot spots within the tumors, and, second, that acetate uptake and metabolism are likely to be much higher in specific types of tumors than in normal human brain tissue. Metabolic data are derived from a small set of tumors, but glioblastoma and meningioma clearly can convert [¹⁴C]acetate into acidic and amino acid metabolites, presumably through the oxidative pathway of the tricarboxylic acid cycle (Fig. 1). Preferential uptake of acetate is not restricted to astrocytic tumors, suggesting a more broad cell-type distribution of the unidentified monocarboxylic acid transporter isoform that confers acetate transport specificity. Thus, the results of this study are consistent with preliminary reports of high [¹¹C]acetate uptake into human brain tumors (27,28) and the use of [¹¹C]acetate imaging of renal (29) and pancreatic (30) disease and nasopharyngeal carcinoma (31). Tumor imaging would extend the widespread use of [¹¹C]acetate in PET studies to the study of oxidative metabolism in normal and diseased myocardial tissue in vivo (32,33).

CONCLUSION

High labeling of glia-derived tumors by acetate supports the working hypothesis that transporter specificity and metabolic substrate preference are cellular properties that should be exploited further for development of tracers that have broad application to the imaging, localization, and classification of human tumors, especially brain tumors of glial origin. Large variations in acetate uptake into various human tumors suggest that it might also be useful for characterizing tumor type and evaluating growth rate and therapeutic intervention by in vivo PET and nuclear MRI.

ACKNOWLEDGMENTS

The authors thank Sharon Farrow for invaluable assistance in scheduling and obtaining the human tumor samples. This study was supported by grant IBN-9728171 from

the National Science Foundation and grants NS36728 and NS38230 from the National Institutes of Health.

REFERENCES

- Greenberg HS, Chandler WF, Sandler HM. *Brain Tumors*. New York, NY: Oxford University Press; 1999:58–77.
- Kendall BE, Hunter JV. Diagnostic imaging of brain tumours. In: Thomas DGT, Graham DI, eds. *Malignant Brain Tumours*. London, U.K.: Springer-Verlag; 1995:221–264.
- Berl S, Clark DD, Schneider D, eds. *Metabolic Compartmentation and Neurotransmission: Relation to Brain Structure and Function*. New York, NY: Plenum Press; 1975.
- Cerdan S, Künnecke B, Seelig J. Cerebral metabolism of [1,2-¹³C₂] acetate as detected by in vivo and in vitro ¹³C NMR. *J Biol Chem*. 1990;265:12916–12926.
- Hassel B, Sonnewald U, Fonnum F. Glial-neuronal interactions as studied by cerebral metabolism of [2-¹³C]acetate and [1-¹³C]glucose: an ex vivo ¹³C NMR spectroscopic study. *J Neurochem*. 1995;64:2773–2782.
- Waniewski RA, Martin DL. Preferential utilization of acetate by astrocytes is attributable to transport. *J Neurosci*. 1998;18:5225–5233.
- Hassel B, Fonnum F. Selective inhibition of glial cell metabolism in vivo by fluorocitrate. *Brain Res*. 1992;576:120–124.
- Sonnewald U, Westergaard N, Schousboe A, Svendsen J, Unsgård G, Petersen SB. Direct demonstration by [¹³C]NMR spectroscopy that glutamine from astrocytes is a precursor for GABA synthesis in neurons. *Neurochem Int*. 1993;22:19–29.
- Zeevalk GD, Davis N, Hyndman AG, Nicklas WJ. Origins of the extracellular glutamate released during total metabolic blockade in the immature retina. *J Neurochem*. 1998;71:2373–2381.
- Dienel GA, Liu K, Popp D, Cruz NF. Enhanced acetate and glucose utilization during graded photic stimulation: neuronal-glial interactions in vivo. In: Blass JP, McDowell FH, eds. *Oxidative/Energy Metabolism in Neurodegenerative Disorders (Annals of the New York Academy of Sciences, Vol. 893)*. New York, NY: New York Academy of Sciences; 1999:279–281.
- Dienel GA, Ball K, Popp D, Drew P, Cruz NF. Metabolic labeling of glial tumors by [¹⁴C]acetate: high tumor-to-tissue ratio compared to [¹⁴C]deoxyglucose. *Soc Neurosci Abstracts*. 2000;26:1733.
- Kobyashi N, Allen N, Clendenen NR, Ko L-W. An improved rat brain-tumor model. *J Neurosurg*. 1980;53:808–815.
- Sokoloff L, Reivich M, Kennedy C, et al. The [¹⁴C]deoxyglucose method for the measurement of local cerebral glucose utilization: theory, procedure, and normal values in the conscious and anesthetized albino rat. *J Neurochem*. 1977;28:897–916.
- Newman GD, Hospod FE, Qi H, Patel H. Effects of dextran on hippocampal brain slice water, extracellular space, calcium kinetics and histology. *J Neurosci Methods*. 1995;61:33–46.
- Passonneau JV, Lowry OH. *Enzymatic Analysis: A Practical Guide*. Totowa, NJ: Humana Press; 1993:71–81.
- Dienel GA, Cruz NF, Mori K, Holden JE, Sokoloff L. Direct measurement of the λ of the lumped constant of the deoxyglucose method in rat brain: determination of the λ and lumped constant from tissue glucose concentration or equilibrium brain/plasma distribution ratio for methylglucose. *J Cereb Blood Flow Metab*. 1991;11:25–34.
- Veech RL, Harris RL, Veloso D, Veech EH. Freeze-blowing: a new technique for the study of brain in vivo. *J Neurochem*. 1973;20:183–188.
- Knowles SE, Jarrett IG, Filsell OH, Ballard FJ. Production and utilization of acetate in mammals. *Biochem J*. 1974;142:401–411.
- Shields AF, Graham MM, Kozawa SM, et al. Contribution of labeled carbon dioxide to PET imaging of carbon-11-labeled compounds. *J Nucl Med*. 1992;33:581–584.
- Cremer JE, Heath DF, Patel AJ, et al. An experimental model of CNS changes associated with chronic liver disease: portocaval anastomosis in the rat. In: Berl S, Clarke DD, Schneider D, eds. *Metabolic Compartmentation and Neurotransmission: Relation to Brain Structure and Function*. New York, NY: Plenum Press; 1975:461–478.
- Berl S, Frigyesi TL. Metabolism of [¹⁴C]leucine and [¹⁴C]acetate in sensorimotor cortex, thalamus, caudate nucleus and cerebellum of the cat. *J Neurochem*. 1968;15:965–970.
- Browning ET, Groppi VE, Kon C. Papaverine, a potent inhibitor of respiration in C-6 astrocytoma cells. *Mol Pharmacol*. 1974;10:175–181.

23. Lust WD, Schwartz JP, Passonneau JV. Glycolytic metabolism in cultured cells of the nervous system. 1. Glucose transport and metabolism in the C-6 glioma cell line. *Mol Cell Biochem.* 1975;8:169–176.
24. van der Sanden BPJ, Rozijn TH, Rijken PFJW, et al. Noninvasive assessment of the functional neovasculature in 9L-glioma growing in rat brain by dynamic ¹H magnetic resonance imaging of gadolinium uptake. *J Cereb Blood Flow Metab.* 2000;20:861–870.
25. van der Sanden BPJ, Heerschap A, Hoofd L, et al. Effect of carbogen breathing on the physiological profile of human glioma xenografts. *Magn Reson Med.* 1999;42:490–499.
26. Bernsen HJ, Rijken PF, Peters JP, et al. Suramin treatment of human glioma xenografts: effects on tumor vasculature and oxygenation status. *J Neurooncol.* 1999;44:129–136.
27. Liu RS, Chaug CP, Chu YK, et al. [C-11]acetate positron emission tomography in the detection of brain tumors: comparison with [F-18]fluorodeoxyglucose [abstract]. *J Nucl Med.* 1997;38(suppl):240P.
28. Liu RS, Chu LS, Chu YK, Yen SH, Liao SQ, Yeh, SH. Does β -oxidation occur in malignant neoplasm? A concurrent [C-11]acetate and [F-18]FMISO study [abstract]. *J Nucl Med.* 1999;40(suppl):239P.
29. Shreve P, Chiao P-C, Humes HD, Schwaiger M, Gross MD. Carbon-11-acetate PET imaging in renal disease. *J Nucl Med.* 1995;36:1595–1601.
30. Shreve PD, Gross MD. Imaging of the pancreas and related diseases with PET carbon-11-acetate. *J Nucl Med.* 1997;38:1305–1310.
31. Yeh SH, Liu RS, Wu LC, Chang CW, Chen KY. ¹¹C-acetate clearance in nasopharyngeal carcinoma. *Nucl Med Commun.* 1999;20:131–134.
32. Hattori N, Tamaki N, Kudoh T, et al. Abnormality of myocardial oxidative metabolism in noninsulin-dependent diabetes mellitus. *J Nucl Med.* 1998;39:1835–1840.
33. Bengel FM, Permanetter B, Ungerer M, Nekolla S, Schwaiger M. Non-invasive estimation of myocardial efficiency using positron emission tomography and carbon-11 acetate: comparison between the normal and failing human heart. *Eur J Nucl Med.* 2000;27:319–326.





The Journal of
NUCLEAR MEDICINE

Preferential Labeling of Glial and Meningial Brain Tumors with [2-¹⁴C]Acetate

Gerald A. Dienel, David Popp, Paul D. Drew, Kelly Ball, Ali Krisht and Nancy F. Cruz

J Nucl Med. 2001;42:1243-1250.

This article and updated information are available at:
<http://jnm.snmjournals.org/content/42/8/1243>

Information about reproducing figures, tables, or other portions of this article can be found online at:
<http://jnm.snmjournals.org/site/misc/permission.xhtml>

Information about subscriptions to JNM can be found at:
<http://jnm.snmjournals.org/site/subscriptions/online.xhtml>

The Journal of Nuclear Medicine is published monthly.
SNMMI | Society of Nuclear Medicine and Molecular Imaging
1850 Samuel Morse Drive, Reston, VA 20190.
(Print ISSN: 0161-5505, Online ISSN: 2159-662X)

© Copyright 2001 SNMMI; all rights reserved.